Cardiac re-entry dynamics & self-termination in DT-MRI based model of Human Foetal Heart[a)]

I.V.Biktasheva,[1, b)] R.A.Anderson,[2] A.V.Holden,[3] E.Pervolaraki,[3] and F.C.Wen[1]
[1)] *Department of Computer Science, University of Liverpool, Liverpool L69 3BX, UK*
[2)] *MRC Centre for Reproductive Health, University of Edinburgh, Edinburgh EH16 4T3, UK*
[3)] *School of Biomedical Sciences, University of Leeds, Leeds LS2 9JT, UK*

(Dated: 14 April 2017)

The effect of heart geometry and anisotropy on cardiac re-entry dynamics and self-termination is studied here in anatomically realistic computer simulations of human foetal heart. 20 weeks of gestational age human foetal heart isotropic and anisotropic anatomy models from diffusion tensor MRI data sets are used in the computer simulations. The fiber orientation angles of the heart were obtained from the DT-MRI primary eigenvalues. In a spatially homogeneous electrophysiological mono domain model with the DT-MRI based heart geometries, we initiate simplified Fitz-Hugh-Nagumo kinetics cardiac re-entry at a prescribed location in a 2D slice, and in the full 3D anatomy model. In a slice of the heart, the MRI based fiber anisotropy changes the re-entry dynamics from pinned to anatomical re-entry. In the full 3D MRI based model, the foetal heart fiber anisotropy changes the re-entry dynamics from a persistent re-entry to the re-entry self-termination.

The effect of the heart anisotropy and anatomy on cardiac re-entry dynamics, although difficult to demonstrate in experiment, is well appreciated[1], and has been studied in simplified mathematical and computer models[2–5]. The BeatBox[6] High Performance Computing (HPC) cardiac electrophysiology computer simulation environment allows direct incorporation of the high resolution DT-MRI heart anatomy data sets into the biophysically and anatomically realistic computer simulations. In the BeatBox *in-silico* model, the anisotropy of the tissue can be switched "on" and "off" to allow for comparison between the anatomically realistic isotropic and anisotropic conduction, in order to see the specific pure anatomy effects, as well as the interplay between the anisotropy and anatomy of an individual heart. In this paper, we present the DT-MRI based anatomy and myofiber structure realistic computer simulation study of cardiac re-entry dynamics in the *in-silico* model of the human foetal heart[7]. We demonstrate that, in a 2D slice of the heart, the realistic fiber anisotropy of the tissue changes cardiac re-entry dynamics from pinned into fast anatomical re-entry. In the full 3D DT-MRI based model, depending on the initial location of the re-entry, the isotropic geometry of the heart might sustain a perpetual re-entry even with a positive filament tension; while the same positive filament tension re-entry initiated at the same location of the foetal heart with the realistic fiber anisotropy self-terminates within seconds.

I. INTRODUCTION

Since the hypothesis over a century ago that cardiac re-entry underlies cardiac arrhythmias[8,9] , and the much later confirmation of the hypothesis in cardiac tissue experiment[10,11],

[a)] As submitted to Chaos: An Interdisciplinary Journal of Nonlinear Science, Focus Issue on the topic of Complex Cardiac Dynamics.
[b)] Also at CEMPS, University of Exeter, Exeter EX4 4QF, UK.
Author to whom correspondence should be addressed; Electronic mail: ivb@liv.ac.uk

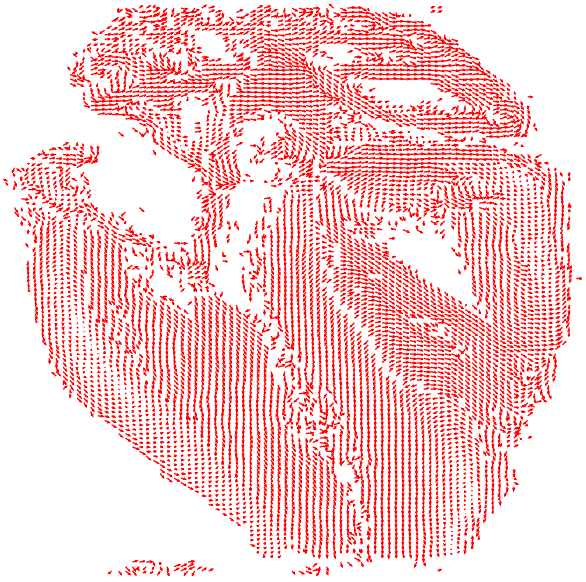

FIG. 1. Formed laminar intramural fibres *vs* chaotic outer-wall regions in a 143 DGA human foetal heart[7], BeatBox[6] geometry `.bbg` format visualisation.

the re-entry (*aka* spiral wave in 2D, cardiac excitation vortex in 3D), its origin and its role in sustained arrhythmias and fibrillation, as well as a possibility of its effective control and defibrillation, have been an object of extensive theoretical study and modelling[2–4,12–24]. From experiment, it is an established point of view that cardiac arrhythmias are due to a complex combination of electrophysiological[25–27], structural[28–31], and anatomical[32,33] factors which sustain cardiac re-entry[34–37].

The specific effect of the heart anisotropy and anatomy on cardiac re-entry dynamics is well appreciated[1], and has been studied in simplified models[2–5]. The recent advance in DT-MRI technology and High Performance Computing (HPC) allows the obtained DT-MRI data sets with the detailed heart anatomy and myofiber structure to be directly incorporated into the anatomically realistic computer simulations[6], so that the anisotropy of the tissue in the *in-silico* model can be switched on and off to allow for comparison between the anatomically realistic isotropic and anisotropic conduction in order to see specific anatomy effects as well as the interplay between the anisotropy and anatomy of an individual heart.

In this paper, we present the DT-MRI based anatomically and myofiber structure realistic computer simulation study of cardiac re-entry dynamics in the *in-silico* model of human foetal heart. We demonstrate that, in a 2D slice of the heart, the realistic fiber anisotropy might change the re-entry dynamics from pinned to anatomical re-entry.

In the full 3D DT-MRI based model, depending on the location of the re-entry initiation, the isotropic geometry of the heart might sustain perpetual re-entry even with a positive filament tension kinetics. While the same positive filament tension re-entry initiated at the same location of the foetal heart with the realistic fiber anisotropy self-terminates within seconds.

II. METHODS

A. DT-MRI based anatomy model

The DT-MRI data sets of the $128\times128\times128$ voxels size, with voxel resolution of $\sim 100\mu m$, of ethically obtained 143 days of gestational age (DGA) human foetal heart[7], were converted

into the BeatBox[6] regular Cartesian mesh `.bbg` geometry format, containing the DT-MRI cartesian coordinates of the heart tissue points together with the corresponding components of the diffusion tensor primary eigenvectors[6]. The `.bbg` file is an ASCII text file, each line in which describes a point in a regular mesh in the following format:

```
x,y,z,status,fibre_x,fibre_y,fibre_z
```

Here `x, y, z` are integer Cartesian coordinates of a DT-MRI voxel, `status` is a flag with a nonzero-value for a tissue point, and `fibre_x, fibre_y, fibre_z` are x-, y- and z-components of the fibre orientation vector at that point. To reduce the size of the `.bbg` files, only the tissue points, that is points with nonzero `status` need to be specified, because the BeatBox solver will ignore the void points with zero status in any case. Although the original DT-MRI images data sets had $128 \times 128 \times 128$ voxels size, the actual dimensions of the foetal heart minimum bounding box were $67 \times 91 \times 128$, with 181070 tissue points.

The DT-MRI based anatomy models were not segmented, only "tissue"/"not tissue" points differentiation were taken into account in the computer simulation of cardiac re-entry dynamics.

The cross section of the DT-MRI based anatomy model in Fig. 1shows that the foetal heart intramural laminar structure was already formed, although the epicardial, endocardial, and between the chambers fibers were yet chaotic. The latter offered a unique opportunity to see if the 20 weeks of gestation age intramural heart structure was capable to support cardiac re-entry, as it would not be possible for the re-entry to pin to the endocardial fine features which were yet to be developed later, such as *e.g.* the pinning to pectinate muscles junction with crystae terminalis reported in adult human atria[35,37,38].

B. Cardiac Tissue Model

To investigate the effects of anatomy on cardiac re-entry dynamics we used *monodomain* tissue model with non-flux boundary conditions

$$\frac{\partial \mathbf{u}}{\partial t} = \mathbf{f}(\mathbf{u}) + \nabla \cdot \hat{\mathbf{D}} \nabla \mathbf{u}, \qquad \vec{n} \cdot \hat{\mathbf{D}} \nabla \mathbf{u} \Big|_G = 0, \tag{1}$$

where $\mathbf{u}(\vec{r}, t) = (u, v)^T$, $\vec{r}$ is the position vector, $\mathbf{f}(\vec{r}, t) = (f, g)^T$ is the Fitz-Hugh-Nagumo[39] kinetics column-vector

$$\begin{aligned} f(u, v) &= \alpha^{-1}(u - u^3/3 - v), \\ g(u, v) &= \alpha\,(u + \beta - \gamma v), \end{aligned} \tag{2}$$

with the parameter values $\alpha = 0.3$, $\beta = 0.68$, $\gamma = 0.5$, which in an infinite excitable medium support a rigidly rotating vortex with positive filament tension[40]; $\hat{\mathbf{D}} = \mathbf{Q}\hat{P}$, where $\mathbf{Q} = \mathrm{diag}(1, 0) = \begin{bmatrix} 1 & 0 \\ 0 & 0 \end{bmatrix}$ is the matrix of the relative diffusion coefficients for u and v components, and $\hat{P} = [P_{jk}] \in \mathbb{R}^{3\times 3}$ is the u component diffusion tensor, which has only two different eigenvalues: the bigger, simple eigenvalue $P_\parallel$ corresponding to the direction along the tissue fibers, and the smaller, double eigenvalue $P_\perp$, corresponding to the directions across the fibres, so that

$$P_{jk} = P_\perp \delta_{jk} + \left(P_\parallel - P_\perp\right) f_j f_k, \tag{3}$$

where $\vec{f} = (f_k)$ is the unit vector of the fiber direction; $\vec{n}$ is the vector normal to the tissue boundary G. In the isotropic simulation, $P_\parallel$ and $P_\perp$ values were fixed at $P_\parallel = P_\perp = 1$. In the anisotropic simulations, $P_\parallel$ and $P_\perp$ values were fixed at $P_\parallel = 2$, $P_\perp = 0.5$.

All the computer simulations presented here were done using the BeatBox[6] software package with the explicit time-step Euler scheme, on the Cartesian regular grid with space step discretization $\Delta x = 0.1$, time step discretisation $\Delta t = 0.001$; 5-point stencil for isotropic, and 9-point stencil for anisotropic Laplacian approximation in 2D simulations; 7-point stencil for isotropic, and 27-point stencil for anisotropic Laplacian approximation in 3D simulations. The re-entry was initiated by the phase distribution method[41]: in the 2D simulations, at a prescribed location of the cross section of the DT-MRI based anatomical model; in the 3D simulations, at a prescribed location of the full DT-MRI based whole heart anatomical model.

III. RESULTS

A. 2D MRI-based "slice" simulations

In the 2D simulations, Fig. 2, a counter-clockwise re-entry was initiated by the phase distribution method[41], with the initial center of rotation placed at the prescribed location $x_0 = 40, y_0 = 60$ in the 2D cross section of the DT-MRI based anatomical model shown in Fig. 1.

In the Fig. 2(a-b), it can be seen that in both isotropic and anisotropic 2D simulations, at $t = 0$, there was identical location of the initial re-entry rotation center: roughly in the middle of the slice, in the vicinity of the septum cuneiform opening.

Fig. 2(a) shows the isotropic dynamics of the re-entry, that is with the fiber orientation data "turned OFF", so that only the geometry of the isotropic homogeneous slice affects the dynamics of the re-entry. While it is known that in an infinite medium the chosen FHN kinetics parameter values $\alpha = 0.3$, $\beta = 0.68$, $\gamma = 0.5$ produce rigidly rotating spiral[39], the anatomically realistic boundaries of the foetal heart cause the drift of the re-entry. The re-entry does not terminate because of the resonant reflection from the inexcitable boundaries[19], but after the transient first rotation around the septum cuneiform opening, the tip of the re-entry firmly pins to the sharp lower end of the cuneiform opening, see Fig. 2(a).

Fig. 2(b) shows the anisotropic dynamics of the re-entry, that is with the fiber orientation data "turned ON", so that both the anatomically realistic geometry and the anisotropy of the otherwise homogeneous slice of the heart affect the dynamics of the re-entry, causing its drift. In the anisotropic slice, the re-entry also does not terminate at the inexcitable boundaries, but after the faster than in the isotropic case, see the *a.u.* time labels in the Fig. 2(a-b), transient first rotation around the septum cuneiform opening, the anatomically realistic anisotropy of the medium turns the initial spiral wave into the fast anatomical re-entry around the septum cuneiform opening, see Fig. 2(b).

B. 3D Whole heart MRI-based simulations

In the 3D whole heart MRI-based simulations shown in the Fig. 3 and Fig. 4, a counter-clockwise excitation vortex was initiated by the phase distribution method[41], with the initial position of the transmural vortex filament (yellow line) at the prescribed location along the x axis at $y_0 = 40, z_0 = 60$.

It can be seen in Fig. 3 and Fig. 4 that in the both the isotropic and the anisotropic 3D simulations, at $t = 0$, there was the identical location of the transmural filament of the excitation vortex: that is transmurally, roughly in the middle through the ventricles of the foetal heart.

Fig. 3 shows the *isotropic dynamics* of the excitation vortex, that is with the fiber orientation data "turned OFF", so that only the geometry of the otherwise isotropic homogeneous foetal heart affects the dynamics of the vortex. It is known that the chosen FHN kinetics

parameter values $\alpha = 0.3$, $\beta = 0.68$, $\gamma = 0.5$ produce rigidly rotating vortex with the positive filament tension[40], which, depending on the topology, either collapses or straightens up between the opposite boundaries of the excitable medium. In the 3D anatomically realistic isotropic simulations of the foetal heart, the anatomically realistic boundaries of the heart cause the drift of the excitation vortex, and, depending on the initial position of the vortex filament, vortices with the positive filament tension tend to collapse. However, there exist initial locations of the excitation vortex, which although result in the drift of the vortex, still do not lead to the expected collapse of the vortex with the positive filament tension. One of such outcomes is shown in the Fig. 3. Here, following the geometry of the heart, after a very short transient the initial vortex filament breaks into the two short pieces each of which finds its own synchronous perpetual pathway, resulting in the perpetual cardiac re-entry in the foetal heart, see Fig. 3.

Fig. 4 shows the *anisotropic dynamics* of the excitation vortex, that is with the fiber orientation data "turned ON", so that both the anatomically realistic geometry and the anisotropy of the otherwise homogeneous foetal heart affect the dynamics of the initial vortex.

In the 3D anatomically realistic simulation of the anisotropic foetal heart, the anisotropy of the heart causes fast transient distortion of the vortex filament and the drift towards the inexcitable boundary of the heart, which ultimately results in the fast self-termination of the excitation vortex, see Fig. 4.

IV. DISCUSSION AND FUTURE DIRECTIONS

Although the role of the heart anatomy and anisotropy in the origin and sustainability of cardiac arrhythmias has been appreciated for a long time, the experimental evidence capable to clarify the detail of the effects of the heart anatomy on the persistent cardiac arrhythmias and fibrillation are limited. Combination of the High Performance Computing with the high-resolution DT-MRI based anatomy models of the heart allows anatomically realistic *in-silico* testing of the effects of individual heart anatomy and anisotropy on the cardiac re-entry dynamics[6,38,42].

In this paper, for the first time, we present the anatomy and myofiber structure realistic computer simulation study of the cardiac re-entry dynamics in the DT-MRI based model of the human foetal heart[7]. The comparative isotropic *vs* anisotropic simulation of the otherwise homogeneous foetal heart shows that, in the 2D slice of the heart, the realistic fiber anisotropy might change the re-entry dynamics from pinning to the sharp end of the septum cuneiform opening, Fig. 2(a), into a fast anatomical re-entry around the opening, Fig. 2(b). In the 3D DT-MRI based *isotropic* model of the foetal heart, depending on the initial location of the organising filament of the excitation vortex, the geometry of the heart on its own might sustain perpetual cardiac re-entry even with a positive filament tension, Fig. 3. However, if the same positive filament tension vortex is initiated at the exactly same location in the full *anisotropic* 3D DT-MRI based model of the heart, the realistic fiber structure of the foetal heart facilitates fast self-termination of cardiac re-entry, Fig. 4.

The BeatBox DT-MRI based *in-silico* model comparative study confirms the cardiac anatomy and anisotropy functional effect on cardiac re-entry sustainability as opposed to its self termination, the pinning of the re-entry to anatomical features, its transformation from pinned to anatomical re-entry, and the re-entry self-termination caused by the anisotropy of the tissue.

One of the limitations of the present study is the use of the simplified Fitz-Hugh-Nagumo[39] excitation model Eq. (2). The simplified FHN model with the excitation kinetics parameters $\alpha = 0.3$, $\beta = 0.68$, $\gamma = 0.5$, which, in an infinite homogeneous isotropic excitable medium, supports a rigidly rotating vortex with positive filament tension[40], was chosen for this study in order to eliminate the effects of realistic cell excitation kinetics, such as *e.g.* meander[39], alternans[43], negative filament tension[40], etc., in order to enhance and highlight the pure effects of the heart anatomy and anisotropy on the cardiac re-entry outcome. The

realistic cell excitation models should be used in the future studies, in order to clarify the particular effects and interplay of the cell excitation kinetics with the heart anatomy and anisotropy.

As it can be seen from Fig. 1, formation of the fiber structure at the epicardium and endocardium is not completed yet in the foetal heart[7], so that only the already formed intramural laminar structure of the fibers can affect the dynamics of cardiac re-entry. Although the use of the not fully formed foetal heart can be seen as a limitation of the study, on the other hand, it may be said that the chaotic epicardium and endocardium fiber orientation prevents the foetal heart re-entry from pinning to the fine anatomical features which were yet to be developed at the endocardium later on, such as *e.g.* the reported pinning of cardiac re-entry to the junction of pectinate muscles with crystae terminalis in adult human atrium[35,37,38]. That is, although it is possible to initiate a cardiac re-entry in the tiny $1.4g$ (at 143 DGA) foetal heart[7], the already formed intramural laminar fiber anisotropy of the foetal heart facilitates the re-entry self-termination, Fig. 4. With the hindsight of the present study, in a fully formed adult heart, because of the presence of the pinning opportunities provided by the endocardium anatomical features[35,37,38], there must exist additional mechanisms to facilitate cardiac re-entry self-termination[44].

The most serious limitation of the study is that the DT-MRI based anatomy model was not segmented, only the "tissue"/"not tissue" points differentiation was taken into account in the BeatBox[6] computer simulation of the cardiac re-entry dynamics, while for sure the heart collagen skeleton would have prevented the re-entry free propagation from ventricles to atria and back. The realistic segmentation of the heart, with the account of the heart collagen skeleton, will inevitably change the outcome of the re-entry, by adding additional electrically impermeable anatomical barriers to the possibility of cardiac re-entry perpetuity shown in Fig. 3. Currently, the realistic tissue segmentation is acquired from DT-MRI data sets via complex image post-processing[45,46], which limits the available segmented DT-MRI cardiac anatomy data sets. In the future, the multichannel computer tomography might offer an automatic tissue segmentation, so that the segmented DT-MRI based heart anatomy models might become more available, and be used in the BeatBox[6] anatomically and biophysically realistic simulations of cardiac re-entry dynamics.

V. SUPPLEMENTARY MATERIAL

Video S1 Movie illustration to Fig. 2(a). (MPG)
Video S2 Movie illustration to Fig. 2(b). (MPG)
Video S3 Movie illustration to Fig. 3. (MPG)
Video S4 Movie illustration to Fig. 4. (MPG)

ACKNOWLEDGMENTS

We acknowledge the support of the UK Medical Research Council grant G1100357 for the human foetal heart DT-MRI data sets. We also wish to acknowledge the support of the BeatBox software development project by EPSRC (UK) grants EP/I029664 and EP/P008690/1. We thank all the developers of the BeatBox HPC Simulation Environment for Biophysically and Anatomically Realistic Cardiac Electrophysiology. We are grateful to Professor V.N.Biktashev for much appreciated advice and discussion.

[1]K. Fukumoto, M. Habibi, S. Ipek, E. G. Zahid, I. M. Khurram, S. L. Zimmerman, V. Zipunnikov, D. Spragg, H. Ashikaga, N. Trayanova, G. F. Tomaselli, J. Rickard, J. E. Marine, R. D. Berger, H. Calkins, and S. Nazarian, "Association of left atrial local conduction velocity with late gadolinium enhancement on cardiac magnetic resonance in patients with atrial fibrillation," CIRCULATION-ARRHYTHMIA AND ELECTROPHYSIOLOGY **9**, e002897 (2016).

[2]F. Fenton and A. Karma, "Vortex dynamics in three-dimensional continuous myocardium with fiber rotation: Filament instability and fibrillation," Chaos **8**, 20–47 (1998).

[3]A. M. Pertsov, M. Wellner, M. Vinson, and J. Jalife, "Topological constraint on scroll wave pinning," Phys. Rev. Lett. **84**, 2738–2741 (2000).
[4]M. Wellner, O. Berenfeld, J. Jalife, and A. M. Pertsov, "Minimal principle for rotor filaments," Proc. Nat. Acad. Sci. USA **99**, 8015–8018 (2002).
[5]B. Rodriguez, J. C. Eason, and N. Trayanova, "Differences between left and right ventricular anatomy determine the types of reentrant circuits induced by an external electric shock. a rabbit heart simulation study," PROGRESS IN BIOPHYSICS & MOLECULAR BIOLOGY **90**, 399–413 (2006).
[6]M. Antonioletti, V. N. Biktashev, A. Jackson, S. R. Kharche, T. Stary, and I. V. Biktasheva, "Beatbox - hpc simulation environment for biophysically and anatomically realistic cardiac electrophysiology," PLoS ONE , *to appear* (2017).
[7]E. Pervolaraki, R. A. Anderson, A. P. Benson, B. Hays-Gill, A. V. Holden, B. J. R. Moore, M. N. Paley, and H. G. Zhang, "Antenatal architecture and activity of the human heart," INTERFACE FOCUS **3**, 20120065 (2013).
[8]G. R. Mines, "On dynamic equilibrium in the heart," J. Physiol. **46**, 349–383 (1913).
[9]W. E. Garey, "The nature of fibrillatory contraction of the heart – its relation to tissue mass and form," Am. J. Physiol. **33**, 397–414 (1914).
[10]M. A. Allessie, F. I. M. Bonke, and F. J. Schopman, Circ. Res. **32**, 54–62 (1973).
[11]A. M. Pertsov, J. M. Davidenko, R. Salomonsz, and J. Baxter, W. T. Jalife, "Spiral waves of excitation underlie reentrant activity in isolated cardiac muscle," Circ. Res. **72**, 631–650 (1993).
[12]N. Wiener and A. Rosenblueth, "The mathematical formulation of the problem of conduction of impulses in a network of connected excitable elements, specifically in cardiac muscle," Arch. Inst. Cardiologia de Mexico **16**, 205–265 (1946).
[13]I. Balakhovsky, "Some regimes of excitation movement in an ideal excitable tissue," Biofizika **9**, 1–63 (1965), in Russian.
[14]V. Krinsky, "Fibrillation in the excitable media," Problemy Kibernetiki **2**, 59–80 (1968), in Russian.
[15]A. V. Panfilov, A. N. Rudenko, and A. M. Pertsov, "Twisted scroll waves in active 3-dimensional media," Doklady AN SSSR **279**, 1000–1002 (1984), in Russian.
[16]V. A. Davydov, V. S. Zykov, A. S. Mikhailov, and P. K. Brazhnik, "Drift and resonance of spiral waves in active media," Radiofizika **31**, 574–582 (1988), in Russian.
[17]J. P. Keener, "The dynamics of three-dimensionsional scroll waves in excitable media," Physica D **31**, 269–276 (1988).
[18]E. A. Ermakova, A. M. Pertsov, and E. E. Shnol, "On the interaction of vortices in 2-dimensional active media," Physica D **40**, 185–195 (1989).
[19]V. N. Biktashev and A. V. Holden, "Design principles of a low-voltage cardiac defibrillator based on the effect of feed-back resonant drift," J. Theor. Biol. **169**, 101–113 (1994).
[20]V. N. Biktashev, "A three-dimensional autowave turbulence," Int. J. of Bifurcation and Chaos **8**, 677–684 (1998).
[21]I. V. Biktasheva and V. N. Biktashev, "Wave-particle dualism of spiral waves dynamics," Phys. Rev. E **67**, 026221 (2003).
[22]V. N. Biktashev, D. Barkley, and I. V. Biktasheva, "Orbital motion of spiral waves in excitable media," Phys Rev Lett **104**, 058302 (2010).
[23]V. N. Biktashev, I. V. Biktasheva, and N. A. Sarvazyan, "Evolution of spiral and scroll waves of excitation in a mathematical model of ischaemic border zone," PLoS ONE **6**, e24388 (2011).
[24]I. V. Biktasheva, H. Dierckx, and V. N. Biktashev, "Drift of scroll waves in thin layers caused by thickness features: asymptotic theory and numerical simulations," Phys. Rev. Lett. **114**, 068302 (2015).
[25]R. F. Bosch and S. Nattel, "Cellular electrophysiology of atrial fibrillation," Cardiovascular Research **54**, 259269 (2002).
[26]A. J. Workman, K. A. Kane, and A. C. Rankin, "Cellular bases for human atrial fibrillation," Heart Rhythm **5**, S1–S6 (2008).
[27]Y. Kushiyama, H. Honjo, R. Niwa, H. Takanari, M. Yamazaki, Y. Takemoto, I. Sakuma, I. Kodama, and K. Kamiya, "Partial i-k1 blockade destabilizes spiral wave rotation center without inducing wave breakup and facilitates termination of reentrant arrhythmias in ventricles," American Journal of Physiology: Heart and Circulatory Physiology **311**, H750–H75 (2016).
[28]J. Pellman, R. C. Lyon, and F. Sheikh, "Extracellular matrix remodeling in atrial fibrosis: mechanisms and implications in atrial fibrillation," Journal of Molecular and Cellular Cardiology **48**, 461467 (2010).
[29]J. Eckstein, B. Maesen, D. Linz, S. Zeemering, A. van Hunnik, S. Verheule, M. Allessie, and U. Schotten, "Time course and mechanisms of endo-epicardial electrical dissociation during atrial fibrillation in the goat," CARDIOVASCULAR RESEARCH **89**, 816–824 (2011).
[30]Y. Takemoto, H. Takanari, H. Honjo, N. Ueda, M. Harada, S. Kato, M. Yamazaki, I. Sakuma, T. Opthof, I. Kodama, and K. Kamiya, "Inhibition of intercellular coupling stabilizes spiral-wave reentry, whereas enhancement of the coupling destabilizes the reentry in favor of early termination," American Journal of Physiology: Heart and Circulatory Physiology **303**, H578H586 (2012).
[31]J. Eckstein, S. Zeemering, D. Linz, B. Maesen, S. Verheule, A. van Hunnik, H. Crijns, M. A. Allessie, and U. Schotten, "Transmural conduction is the predominant mechanism of breakthrough during atrial fibrillation: Evidence from simultaneous endo-epicardial high-density activation mapping," Circulation: Arrhythmia and Electrophysiology **6**, 334341 (2013).
[32]P. G. MacEdo, S. Kapa, J. A. Mears, A. Fratianni, and S. J. Asirvatham, "Correlative anatomy for the

electrophysiologist: ablation for atrial fibrillation. part ii: regional anatomy of the atria and relevance to damage of adjacent structures during af ablation," Journal of Cardiovascular Electrophysiology **21**, 829836 (2010).

[33]M. Anselmino, A. Blandino, S. Beninati, C. Rovera, C. Boffano, M. Belletti, D. Caponi, M. Scaglione, F. Cesarani, and F. Gaita, "Morphologic analysis of left atrial anatomy by magnetic resonance angiography in patients with atrial fibrillation: a large single center experience," Journal of Cardiovascular Electrophysiology **22**, 1–7 (2011).

[34]R. A. Gray, A. M. Pertsov, and J. Jalife, "Incomplete reentry and epicardial breakthrough patterns during atrial fibrillation in the sheep heart," Circulation **94**, 26492661 (1996).

[35]T. J. Wu, M. Yashima, F. Xie, C. A. Athill, Y. H. Kim, M. C. Fishbein, Z. Qu, A. Garfinkel, J. N. Weiss, H. S. Karagueuzian, and P. S. Chen, "Role of pectinate muscle bundles in the generation and maintenance of intra-atrial reentry. potential implications for the mechanism of conversion between atrial fibrillation and atrial flutter," Circulation Research **83**, 448–462 (1998).

[36]S. Nattel, "New ideas about atrial fibrillation 50 years on," Nature **415**, 219226 (2002).

[37]M. Yamazaki, S. Mironov, C. Taravant, J. Brec, L. M. Vaquero, K. Bandaru, U. M. R. Avula, H. Honjo, I. Kodama, O. Berenfeld, and J. Kalifa, "Heterogeneous atrial wall thickness and stretch promote scroll waves anchoring during atrial fibrillation," Cardiovascular Research **94**, 48–57 (2012).

[38]S. R. Kharche, I. V. Biktasheva, G. Seeman, H. Zhang, and V. N. Biktashev, "A computer simulation study of anatomy induced drift of spiral waves in the human atrium," BioMed Research International **2015**, 731386 (2015).

[39]A. T. Winfree, "Varieties of spiral wave behaviour — an experimentalist's approach to the theory of excitable media," Chaos **1**, 303–334 (1991).

[40]V. N. Biktashev, A. V. Holden, and H. Zhang, "Tension of organizing filaments of scroll waves," Phil. Trans. Roy. Soc. Lond. ser. A **347**, 611–630 (1994).

[41]V. N. Biktashev and A. Holden, "Re-entrant waves and their elimination in a model of mammalian ventricular tissue," Chaos **8**, 48–56 (1998).

[42]S. R. Kharche, I. V. Biktasheva, G. Seemann, H. Zhang, J. Zhao, and V. N. Biktashev, "Computational modelling of low voltage resonant drift of scroll waves in the realistic human atria," Lecture Notes in Computer Science **9126**, 421–429 (2015).

[43]A. Karma, "Electrical alternans and spiral wave breakup in cardiac tissue," CHAOS **4**, 461–472 (1994).

[44]R. Clayton, A. Murray, P. Higham, and R. Campbell, "Self-terminating ventricular tachyarrhythmias - a diagnostic dilemma," LANCET **341**, 93–95 (1993).

[45]H. Lombaert, J. Peyrat, P. Croisille, S. Rapacchi, L. Fanton, F. Cheriet, P. Clarysse, I. Magnin, H. Delingette, and N. Ayache, "Human atlas of the cardiac fiber architecture: Study on a healthy population," IEEE TRANSACTIONS ON MEDICAL IMAGING **31**, 1436–1447 (2012).

[46]J. K. Gahm, G. L. Kung, and D. B. Ennis, "Weighted component-based tensor distance applied to graph-based segmentation of cardiac dt-mri," in *2013 IEEE 10TH INTERNATIONAL SYMPOSIUM ON BIOMEDICAL IMAGING (ISBI)*, IEEE International Symposium on Biomedical Imaging (2013) pp. 504–507.

FIG. 2. **Anisotropy effect in the 2D slice simulations**, time shown in arbitrary time units under each panel. **a)** *Isotropic conduction*: after the transient first rotation around the septum cuneiform opening, the slow excitation re-entry pins to the sharp low end of the opening in the foetal heart; see also movie S1 in the Supplementary Material section V; **b)** *Anisotropic conduction*: after the fast transient first rotation around the septum cuneiform opening, the anisotropy of the foetal heart turns the initial spiral wave into the fast anatomical re-entry around the septum cuneiform opening; see also movie S2 in the Supplementary Material section V.

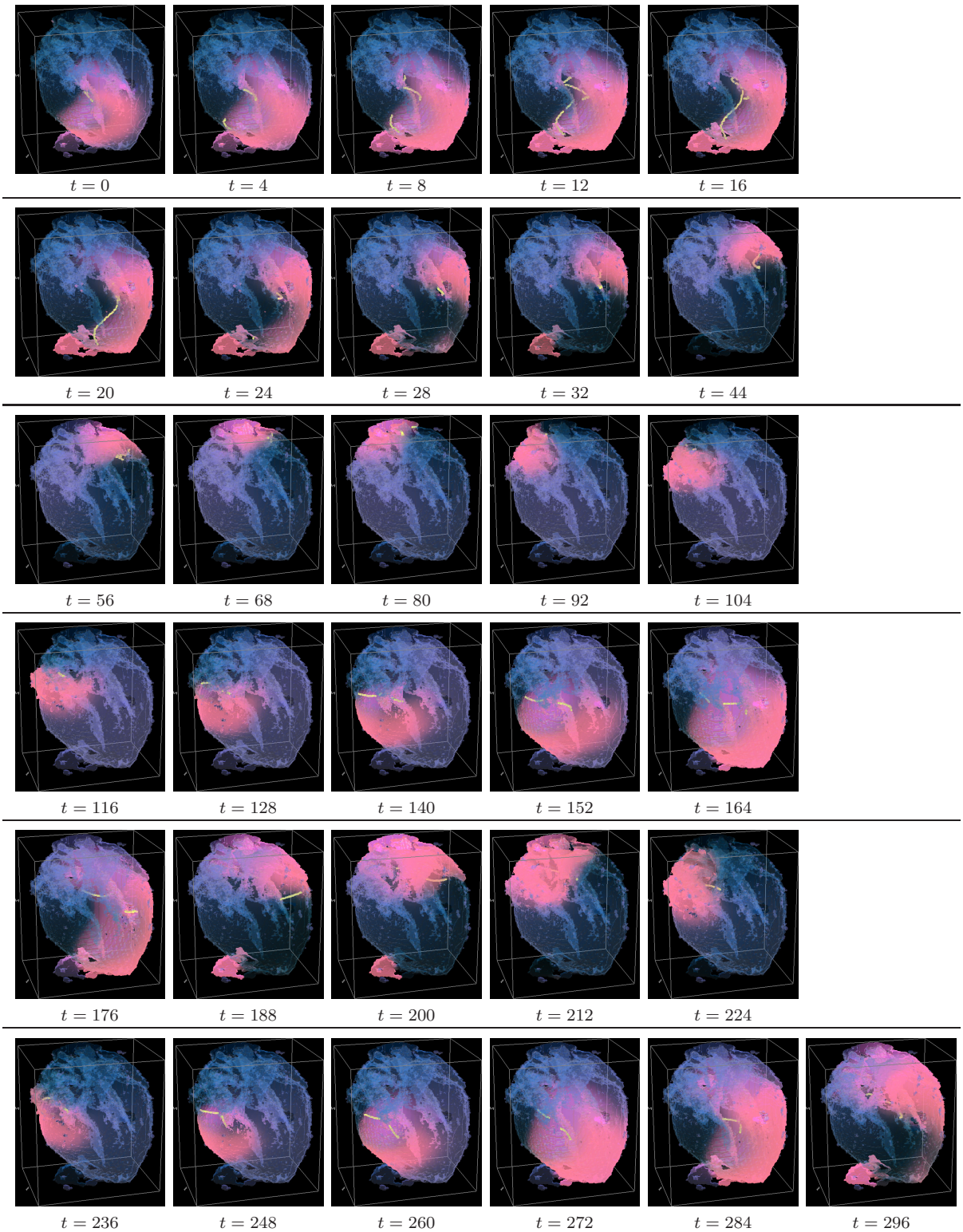

FIG. 3. **Isotropic whole heart simulation.** The translucent foetal heart is shown in blue, excitation front shown in red, the yellow lines are the instant organising filaments of the excitation vortices; time shown in arbitrary time units under each panel. After a short transient the organising filament of the initial vortex breaks into the two short pieces each of which finds its own synchronous perpetual pathway, resulting in the perpetual cardiac re-entry in the foetal heart. See also movie S3 in the Supplementary Material section V.

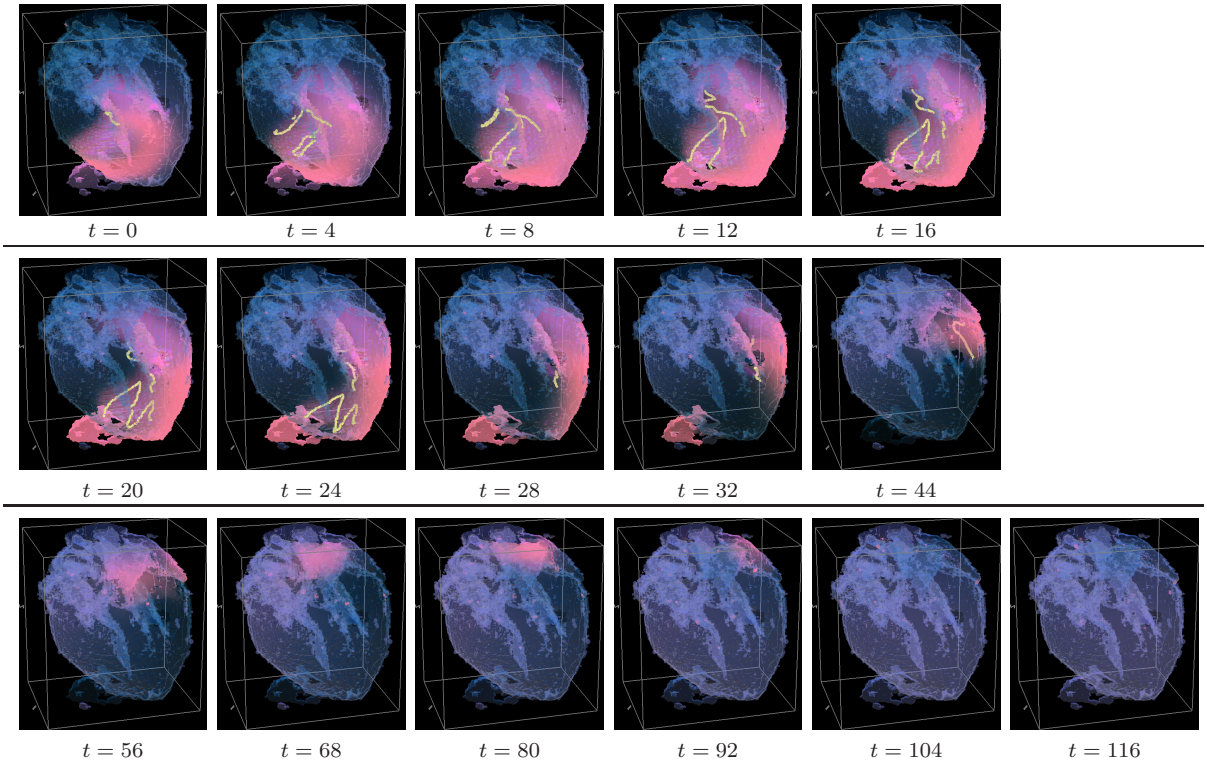

FIG. 4. **Anisotropic whole heart simulation.** The translucent foetal heart is shown in blue, excitation front shown in red, the yellow lines are the instant organising filaments of the excitation vortices; time shown in arbitrary time units under each panel. The anisotropy of the heart causes the fast transient distortion of the organising filament of the initial excitation vortex and drift towards the inexcitable boundary of the heart, ultimately resulting in the very fast self termination of the excitation vortex. See also movie S4 in the Supplementary Material section V.